Hollow Polymer Microneedle Array Fabricated by Photolithography Process Combined with Micromolding Technique

Po-Chun Wang, Brock A. Wester, Swaminathan Rajaraman, Seung-Joon Paik, Seong-Hyok Kim, and
Mark G. Allen

Abstract—**Transdermal drug delivery through microneedles is a minimally invasive procedure causing little or no pain, and is a potentially attractive alternative to intramuscular and subdermal drug delivery methods. This paper demonstrates the fabrication of a hollow microneedle array using a polymer-based process combining UV photolithography and replica molding techniques. The key characteristic of the proposed fabrication process is to define a hollow lumen for microfluidic access via photopatterning, allowing a batch process as well as high throughput. A hollow SU-8 microneedle array, consisting of 825μm tall and 400 μm wide microneedles with 15-25 μm tip diameters and 120 μm diameter hollow lumens was designed, fabricated and characterized.**

I. INTRODUCTION

DRUG delivery through micro-fabricated needles is of great interest for its capability to transport pharmaceutical and therapeutic agents, virus-like-particles, and other molecules into the body through the skin with minimal invasion and pain [1]. A variety of two-dimensional (2D) and three-dimensional (3D) microneedle devices for drug delivery applications have been reported in literature, and typically they contain either solid or hollow microneedles [1-15]. Successfully fabricated solid microneedle devices have been composed of a variety of materials, including silicon [3], metal [4], and polymers [5]. A solid microneedle array with an integrated microelectrode array (MEA) to monitor electrical activity of cells and tissues has also been demonstrated [6].

For manufacturing hollow microneedles, several successful fabrication techniques have been reported. Laser micromachining has been employed to create 400-800 μm tall hollow microneedles by drilling trenches in dissolvable molds to create lumens through microneedle structures [7-9]. Hollow microneedles with 400-700 μm heights and

ultra-sharp tips were achieved using silicon-based MEMS techniques, including anisotropic and isotropic reactive ion etching (RIE) processes and dicing [10, 11]. Integrated lithographic molding techniques using photosensitive polymer and surface micromachined silicon mold were also reported to fabricate 400-450 μm tall hollow microneedles [12, 13]. Other researchers also reported 400 μm tall hollow microneedles by utilizing deep X-ray photolithography and polymethyl-methacrylate (PMMA) as well as metal casting on recessed SU-8 structure [14, 15].

Despite these successes, cost of manufacturing and administration, and volume of drug delivery are major barriers for instruments in this market. The most common approach of drug delivery for solid microneedle arrays is to pre-coat the surface of microneedles to allow contact absorption and diffusion into the dermis following insertion [1, 2]. However, the volume and time of delivery and variety of drug coating compositions in solid microneedle devices are all constrained by limitations in coating technology. 2D devices, which usually contain solid microneedles, offer the lowest costs through reduced manufacturing complexity, but have limited needle surface area for drug coatings. Alternative 3D microneedle arrays are attractive since they contain more needles and thus can deliver higher volumes of drug, but they require more complex fabrication processing. Compared to their solid counterparts, hollow microneedle devices deliver larger drug volumes in a fashion that is similar to conventional hypodermal needles, and typically have faster delivery rates by utilizing the active fluid flow into skin (Fig. 1), but given the dimensional considerations of microsized needle arrays, they historically require expensive manufacturing and packaging processes [1, 2].

This paper proposes the novel fabrication of a 3D hollow microneedle array system with 825 μm tall needles using replica molding and photolithography techniques. Taller microneedles are possible to compensate the skin indentation during the insertion of the array. [16] Combining these techniques provides the means to create a single mold, double exposure photolithography batch process that is scalable and can result in high throughput. The proposed fabrication process utilizes polymer materials, i.e. SU-8 for the patterned hollow microneedle structure and polydimethylsiloxane (PDMS) as an intermediate molding material. This microneedle system, consisting of a hollow microneedle array and a drug reservoir, is depicted in Fig. 1a. Upon the application of external pressure on the reservoir, the

microneedle system is propelled toward and penetrates into the skin, followed by the fluid drug being driven through the lumens and into the skin (Fig. 1b).

This proposed fabrication technique can serve as a platform for low cost microneedle device production that is mass-manufacturable, providing the potential capability to supply annual influenza inoculations as well as mass-immunization efforts against pandemic disease.
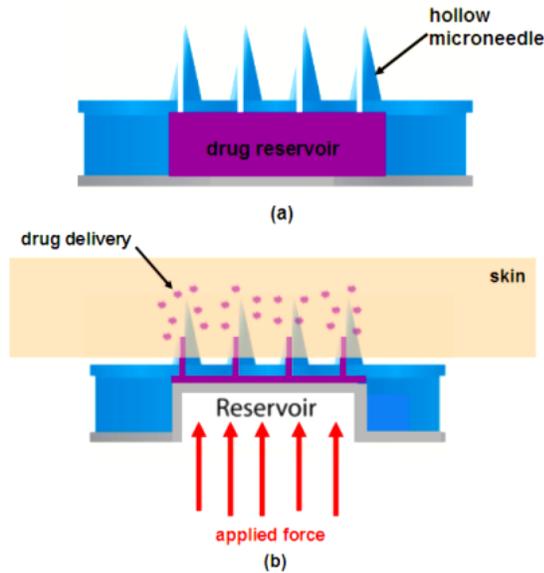

Fig. 1. (a) A schematic depict of the microneedle system, consisting of a hollow microneedle array and a drug reservoir. (b) An illustration of self-administration of drug delivery, showing a pressure is applied upon the microneedle system, leading to the insertion of the microneedles into the skin and the introduction of drug in the skin.

II. FABRICATION

A schematic illustration of desired hollow microneedle is shown in Fig. 2. The hollow microneedle array has three major components: the top pyramidal tip, the square shaft, and the base plate. The lumen of the hollow microneedle has two openings: one is on the pyramidal slope, and the other is located on the bottom side of base plate (Fig. 2b).
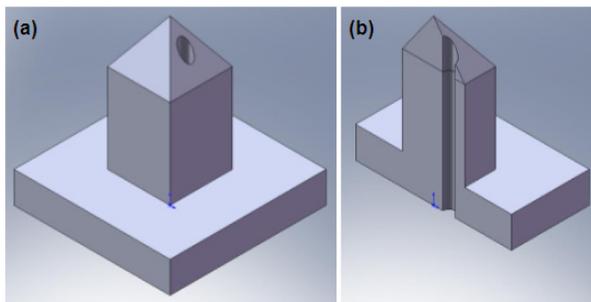

Fig. 2. (a) A depiction showing the desired hollow microneedle structure with a base plate. (b) A cross-sectional view of the hollow microneedle structure, showing the lumen has two openings and connects from the base plate to the top pyramidal slope.

The hollow microneedle array is fabricated in two steps. The first step is to construct an intermediate PDMS mold, which defines profile of the pyramidal tip. The intermediate PDMS mold was fabricated using previously described techniques [17]. The second step is to fabricate the hollow SU-8 microneedle on the constructed intermediate PDMS mold. Fig. 3 illustrates the fabrication steps of hollow SU-8 microneedle array on the intermediate PDMS mold. The SU-8 2025 was first preheated at 60°C for 30 minutes in order to increase its encapsulation of the micro-trenches by reducing its viscosity. The surface of intermediate PDMS mold was treated using oxygen plasma for 20 minutes, which provides more hydrophilic surface for better encapsulation of the micro-trenches (Fig. 3a). The SU-8 was cast by weight to obtain a thickness of 800 μm on the PDMS. A backside vacuuming (BSV) process was performed for 3 hours to remove the bubbles trapped in the PDMS trenches, while maintaining the integrity of the SU-8 top surface (Fig. 3b). The SU-8/PDMS sample was then softbaked at 115°C for 24 hours.
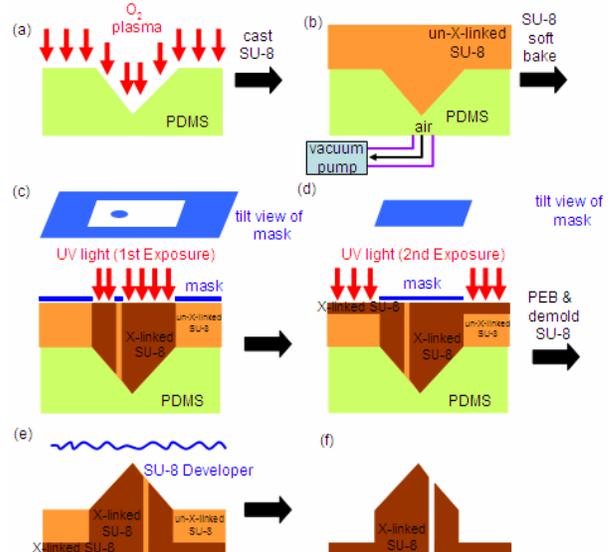

Fig. 3. Process flow for fabrication of hollow SU-8 microneedle array.

The UV (365 nm i-line) photolithography was utilized to define the hollow microneedle structure. Fig. 3c-d illustrates the two straight UV exposures with separate masks. In the first exposure (Fig. 3c), the pyramidal tip and shaft of the hollow microneedle were defined by a chromium mask, consisting of a 400×400 μm^2 clear square region for the shaft and a dark circular pattern of 120 μm in diameter for the lumen. The UV dosage of the process was 3000 mJ. In addition to this intended exposure, an undesirable exposure may occur due to the mismatch in the refractive indices of SU-8 and PDMS. This exposure of SU-8 may lead to undesired crosslinking in the lumen, inhibiting flow. According to Fresnel's equation [18], a lower incident angle of UV light on the SU-8/PDMS interface leads to less

reflection of UV light from the interface (Fig. 3c). Therefore, the inclined angle of the trenches in the PDMS mold was carefully considered. The second exposure with reduced dosage of 350 mJ defines the base plate for the hollow microneedle array (Fig. 3d). A post-exposure-bake (PEB) process was performed to accommodate a certain thickness (350-400 μm) of the base plate.

The SU-8 master was then demolded from the intermediate PDMS mold. The development process and completed SU-8 hollow microneedle are shown in Fig. 3e and 3f, respectively. The development of the SU-8 master in the propylene glycol methyl ether acetate (PGMEA) developer is a two-step process. The first step is development of SU-8 in a static PGMEA bath for 6 hours. The second step is development of SU-8 in an ultrasonic bath for 2 hours in order to remove the clogging in the needle lumens. Following development, the sample was rinsed by isopropyl alcohol (IPA) solution and blown dried by nitrogen gun.

An optical micrograph of fabricated hollow microneedle array is shown in Fig. 4. Each microneedle in the array has a base width of 400 μm, and a height of 825 μm which includes a 255 μm tall pyramidal tip and a 570 μm tall shaft. The chip dimension is 25.6×25.6 mm, with 100 microneedles in the 10×10 array at the center. Fig. 5 shows SEM images of the microneedle array (a), upper shaft with lumen opening (b), and pyramidal tip (c). The tip diameter was measured and shown to range from 15 to 25 μm across the array.
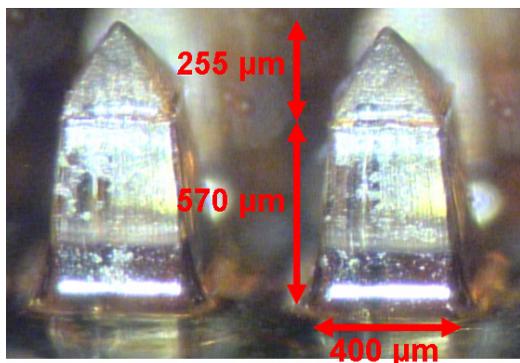

Fig. 4. An optical micrograph showing the fabricated hollow microneedles. Two microneedles from one row of the array are shown

III. TESTING

The qualitative and quantitative functional capacity of the fabricated microfluidic lumens were characterized using a custom fluidic test setup (Fig. 6). The test setup consists of a syringe pump system with a dye filled syringe (food coloring with deionized water) and polymer tubing attaching the syringe to the packaged microneedle array. The testing package consists of a housing with a reservoir, which was attached to the microneedle array using a layer of PDMS. This syringe pump system examined the successful development and formation of the microneedle lumens by flowing dye from the syringe to the microneedle reservoir and

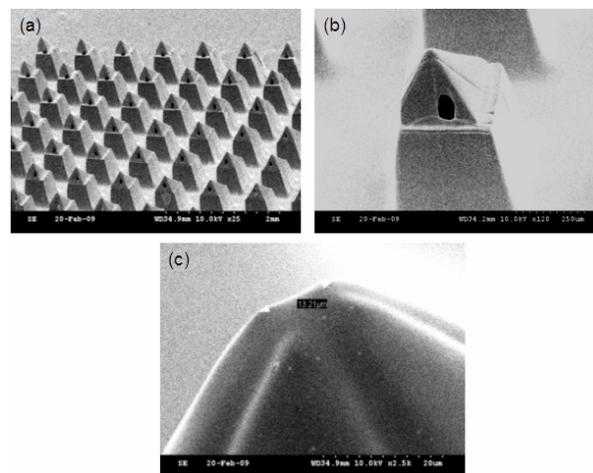then, through any open microneedle lumens.

Fig. 5. (a) A SEM image of bird-eye's view of fabricated microneedle array coated by 15 nm Cr/150 nm Au for SEM imaging. (b) A SEM image revealing the pyramidal tip with a lumen opening and upper shaft. (c) A high magnification (2.5K×) SEM image of the tip of the pyramid. The tip diameter for this microneedle is 13.2 μm, while the tip diameter generally ranges from 15 to 25 μm across the array.
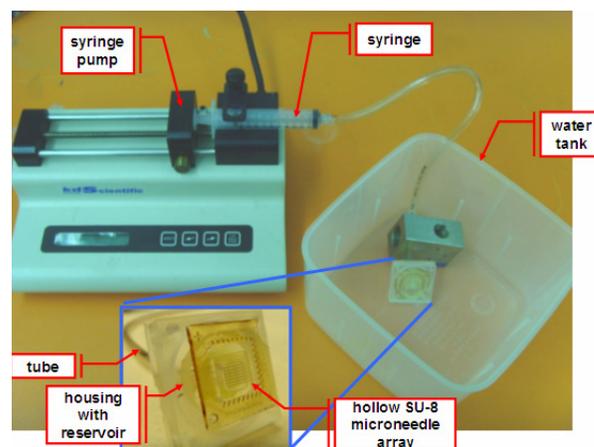

Fig. 6. An optical picture showing the custom fluidic test setup.

The microfluidic characterization was performed both in fresh water and in air. Blue dye was successfully ejected through the lumens of the microneedles while both submersed in water and suspended in air (Fig. 7). Visual inspection of the fluidic ejection from the microneedle array indicated successful lumen formation in one of the 10×10 microneedle array prior to ultrasonic treatment, and ~20 of the array following treatment. (Fig. 7(b)) During fluidic testing, the driving rate on the syringe pump could be increased to 125 mL/h without introducing any visible damage to the microneedle array. The 125 mL/h is the maximum driving rate that the syringe pump can provide through the 6 mL syringe. Manual driving of the dye through microneedle array produced no observable damage.

Microscopic inspection of the microneedle tips and the base plate during the microfluidic characterization confirmed no cracking formation in the base plate and open lumens all the way to the top of the microneedle (Fig. 8). This alleviates concern that base plate cracking is the reason for the observed microfluidic flow.
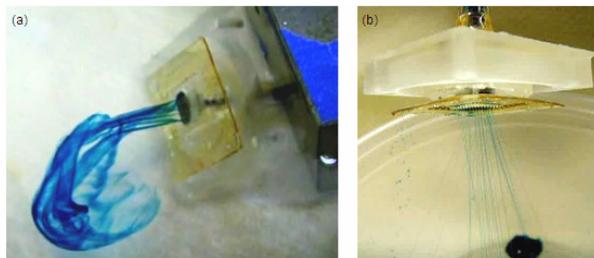

Fig. 7. (a) An optical picture showing the result of fluidic characterization performed in fresh water. Blue dyes were being ejected from the microneedle array. (b) An optical picture illustrating the blue dye being emitted from the array, while the array is suspended in air with microneedles facing down.
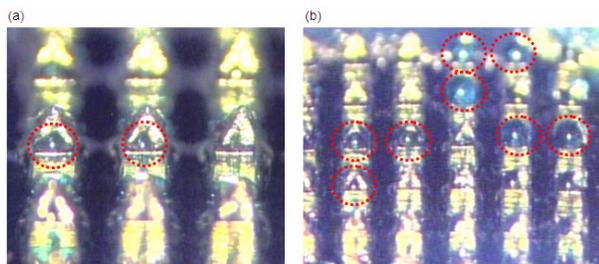

Fig. 8. Images captured from video clips of continuous fluidic characterization recorded by the stereoscope. The images are captured at the moment immediately after the blue dye droplets, which are highlighted by the red dashed circles, were being ejected from the lumens.

IV. CONCLUSION

A polymer-based process integrating UV photolithography and replica molding technique was proposed to fabricate hollow SU-8 microneedle array. A 10×10 array with 825 µm tall microneedles and 15-25 µm tip diameters was successfully fabricated. Following iterative fluidic tests, a yield improvement process for 20% lumen formation was successfully determined.

One key characteristic of this process is that the microfluidic ports in the hollow microneedles are defined by conventional photolithography technique, which is a batch process that inherently allows for high throughput. Other characteristics include taller-than-800µm structures and utilization of potential low cost polymer (SU-8 or PDMS) for final hollow microneedles and intermediate molds. While fabrication outcome and preliminary fluidic tests were demonstrated, additional mechanical and fluidic characterization using penetration and absorption tests with porcine skin are required to assess the efficacy of drug delivery into skin.

References

[1] M. Prausnitz, "Microneedles for transdermal drug delivery," *Adv. Drug Deliv. Rev.*, vol. 56, no. 5, pp. 581–587, Mar. 2004.

[2] E. Nuxoll, R. Siegel, "BioMEMS devices for drug delivery," *IEEE Engineering in Medicine and Biology Mgn.*, vol. 28, pp. 31-39, Jan-Feb 2009.

[3] P. Griss, P. Enoksson, H. K. Tolvanen-Laakso, P. Meriläinen, S. Ollmar, and G. Stemme, "Micromachined electrodes for biopotential measurements," *J. of Microelectromechanical Systems*, vol. 10, pp. 10-16, 2001.

[4] W. Martanto, S. P. Davis, N. R. Holliday, J. Wang, H. S. Gill, and M. R. Prausnitz, "Transdermal delivery of insulin using microneedles in vivo," *Pharmceutical Research*, vol. 21, pp. 947-952, 2004.

[5] J.-H. Park, M. G. Allen, and M. R. Prausnitz, "Biodegradable polymer microneedles: fabrication, mechanics and transdermal drug delivery," *J. of Controlled Release*, vol. 104, pp. 51-66, 2005.

[6] S. Rajaraman, S.-O Choi, R. H. Shafer, J. D. Ross, J. Vukasinovic, Y.-S. Choi, S. P. DeWeerth, A. Glezer and M. G Allen, "Microfabrication technologies for a coupled three-dimensional microelectrode, microfluidic array," *J. Micromech. Microeng.,* vol. 17, pp. 163-171, 2007.

[7] S. P. Davis, W. Martanto, M. G. Allen, and M. R. Prausnitz, "Hollow metal microneedles for insulin delivery to diabetic rats," *IEEE Trans. Biomed. Eng.*, vol. 52, pp. 909-915, 2005.

[8] Y.-S. Choi, M. A. McClain, M. C. LaPlaca, A. B. Frazier, and M. G. Allen, "Three dimensional MEMS microfluidic perfusion system for thick brain slice cultures," *Biomed. Microdevices*, vol. 9, pp. 7-13, 2007.

[9] A. Ovsianikov, B. Chichkov, P. Mente, N. A. Monteiro-Riviere, A. Doraiswamy, and R. J. Narayan, " Two photon polymerization of polymer-ceramic hybrid materials for transdermal drug delivery," *Int. J. Appl. Ceram. Technol.*, vol. 4, pp. 22-29, 2007.

[10] N. Roxhed, T. C. Gasser, P. Griss, G. A. Holzapfel, and G. Stemme, "Penetration-enhanced ultrasharp microneedles and prediction on skin interaction for efficient transdermal drug delivery," *J. Microelectromechanical Sys.*, vol. 16, pp. 1429-1440, 2007.

[11] N. Baron, J. Passave, B. Guichardaz, and G. Cabodevila, "Investigations of development process of high hollow beveled microneedles using a combination of ICP RIE and dicing saw," *Microsyst. Technol.*, vol. 14, pp. 1475-1480, 2008.

[12] R. Luttage, E. J. W. Berenschot, M. J. de Boer, D. M. Altpeter, E. X. Vrouwe, A. van den Berg, and M. Elwenspoek, "Integrated lithographic molding for microneedle-based devices," *J. Microelectromechanical Sys.*, vol. 16, pp. 872-884, 2007.

[13] S.-C. Kuo, and Y. Chou, "A novel polymer microneedle arrays and PDMS micromolding technique," *Tamkang J. Sci. Eng.*, vol. 7, pp. 95-98, 2004.

[14] F. Perennes, B. Marmiroli, M. Matteucci, M. Tormen, L. Vaccari, and E. D. Fabrizio, "Sharp beveled tip hollow microneedle arrays fabricated by LIGA and 3D soft lithography with polyvinyl alcohol," *J. Micromech. Microeng.*, vol. 16, pp. 473-479, 2006.

[15] K. Kim, D. S. Park, H. M. Lu, W. Che, K. Kim, J.-B. Lee, and C. H. Ahn, "A tapered hollow metallic microneedle array using backside exposure of SU-8," *J. Micromech. Microeng.*, vol. 14, pp. 597-603, 2004

[16] W. Martanto, J. S. Moore, T. Couse, M. R. Prausnite, "Mechanism of Fluid Infusion During Microneedle Insertion and Retraction," *J. Controlled Release*, vol. 112, pp. 357-361, 2006.

[17] S. Rajaraman, M. A. McClain, S.-O Choi, J. D. Ross, S. P. DeWeerth, M. C. LaPlaca, and M. G. Allen, "Three-Dimensional Metal Transfer Micromolded Microelectrode Arrays (MEAS) For In-Vitro Brain Slice Recordings," *Proc. Transducers 2007: The 14th Int. Conf. on Solid-State Sensors, Actuators and Microsystems*, pp.1251-1254, Lyon, France, June 10-14, 2007.

[18] M. S. Rogalski, S. B. Palmer, *Advanced University Physics.* Boca Raton, FL: CRC Press, 2005, pp. 411-428.